RSC Advances

PAPER

View Article Online
View Journal | View Issue

Cite this: *RSC Adv.*, 2017, **7**, 6492

Optimizing photovoltaic performance in $CuInS_2$ and CdS quantum dot-sensitized solar cells by using an agar-based gel polymer electrolyte†

E. Raphael,[ab] D. H. Jara[b] and M. A. Schiavon*[a]

Received 1st December 2016
Accepted 9th January 2017

DOI: 10.1039/c6ra27635k

www.rsc.org/advances

Quantum dot-sensitized solar cells (QDSSCs) offer new opportunities to address the clean energy challenge, being one of the top candidates for third generation photovoltaics. Like dye-sensitized solar cells (DSSCs), QDSSCs normally use liquid electrolytes that suffer from issues such as evaporation or leakage. In this study a gel polysulfide electrolyte was prepared containing a natural polymer, agar, and was used as a quasi-solid-state electrolyte in solar cells to replace the conventional liquid electrolytes. This gel electrolyte shows almost the same conductivity as the liquid one. The solar cells were fabricated using $CuInS_2$ quantum dots (QDs), previously synthesized, deposited on TiO_2 photoanodes by electrophoretic deposition (EPD). CdS was deposited on TiO_2 by successive ionic layer adsorption and reaction (SILAR). Reduced graphene oxide (RGO)–Cu_2S, brass, and thin film Cu_xS were used as counter electrodes. Compared to a liquid polysulfide water based electrolyte, solar cells based on $CuInS_2$ and CdS using gel polymer electrolyte (GPE) exhibit greater incident photon to current conversion efficiency (IPCE = 51.7% at 520 nm and 72.7% at 440 nm), photocurrent density (J_{sc} = 10.75 and 13.51 mA cm^{-2}), and power conversion efficiency (η = 2.97 and 2.98%) while exhibiting significantly enhanced stability. The solar cells employing the agar-based gel polymeric electrolyte are about a factor of 0.20 more stable than using a liquid electrolyte. The higher photovoltaic performance is due to the good conductivity and high wettability as well as the superior permeation capability of the gel electrolyte into the mesoporous matrix of a TiO_2 film.

Introduction

The worldwide demand for energy is increasing. The production, storage and distribution of energy are necessities of industry and society, and because of limited fossil fuel reserves on the planet, reliable and alternative renewable energy sources are becoming increasingly important areas of interest.[1] Quantum dot (QD)-sensitized solar cells (QDSSCs), as an alternative to dye-sensitized solar cells (DSSCs), have been of focus in research because of their efficient charge separation and transport,[2] offering new opportunities to address the clean energy challenge.[3,4] Quantum dots (QDs) are semiconductor nanocrystals in which quantum confinement occurs. They usually have diameters in the range of 2–10 nanometers and their size tunability drastically affects the optical and electronic properties, which in turn have a strong impact on their performance in devices such as photovoltaics.[5,6] Different deposition techniques like: Chemical Bath Deposition (CBD), QD functionalization, Close Space Sublimation (CSS), Successive Ion Layer Adsorption and Reaction (SILAR), Metal Organic Chemical Vapor Deposition (MOCVD), Vapor Phase Epitaxy (VPE), and electrophoretic deposition (EPD) have been used to deposit the absorber layer onto mesoscopic oxide (*e.g.*, TiO_2) films.[3,4,7] QDSSCs typically exhibit lower power conversion efficiency when comparable to DSSCs or thin film solar cells, however, their efficiency has considerably increased from 1% to over 8%. Factors that limit the overall power conversion efficiency is the limited harvesting of the incident light, slow hole transfer rate, back electron transfer to the redox couple, or low counter electrode performance.[8–10] In order to improve the efficiency, it is necessary to explore new approaches to different aspects such as different electrolytes. In a conventional QDSSC the redox electrolyte is located between the working and counter electrodes and plays an important role in regenerating the semiconductor by scavenging photogenerated holes and determines the photovoltage of the liquid junction solar cells.[11] Organic-solvent-based liquid electrolytes have been conventionally used, but due to the toxicity of several organic solvents, water-based electrolytes are being employed. The aqueous cells are environmentally friendly,[12] but the efficiency and stability of the cells in an aqueous phase have been low.[13] The liquid

[a]*Department of Natural Science, Federal University of São João del-Rei – UFSJ, São João del-Rei, Minas Gerais 36301-160, Brazil. E-mail: schiavon@ufsj.edu.br*
[b]*Radiation Laboratory, Department of Chemistry and Biochemistry, University of Notre Dame, Notre Dame, Indiana 46556, USA*

† Electronic supplementary information (ESI) available. See DOI: 10.1039/c6ra27635k

sulfide/polysulfide redox electrolyte has remained a preferred choice because it assists in delivering high open circuit voltage and stability of solar cell operation. The I^-/I^{3-} redox couple, traditionally used in DSSCs, is corrosive to QDs, causing a decrease in photocurrent.[14] However, liquid electrolytes have a fundamental limitation for long-term operation due to their volatilization and leakage due to inadequate sealing of cells, possible desorption, and photodegradation of the sensitizer.[12,15,16] Therefore, a development of new materials to replace traditional liquid electrolytes is essential. Polymer electrolytes are nowadays the focus of researches. One method to make these electrolytes is to alter the physical-chemistry properties of these polymeric materials by addition of plasticizers to obtain gel polymeric electrolytes (GPE). The plasticizer influences the thermal and mechanical properties and attains sufficient penetration of the polymer electrolyte into the porous photoelectrode.[17,18] GPEs have recently received considerable attention because they can be prepared in a semisolid or solid form, they are cheap, acquire liquid-like conductivity (10^{-2} to 10^{-3} S cm^{-1}), have superior mechanical properties and promise long-term stability.[16,19,20] With these properties, GPEs can be applied in devices such as fuel cells, electrochromic devices, sensors, batteries and solar cells.[21] However, a common feature related to most solar cells prepared with polymer electrolyte is the notable reduction in efficiency primarily due to the lower mobility of the ionic species through the solid or quasi-solid medium, or poor wetting of pores with the electrolyte. The conversion efficiencies with the gel polymer electrolytes typically is low, but even at low efficiencies, these cells have been viable alternatives to the generally liquid electrolyte used in DSSCs or QDSSCs due to improved stability and better sealing ability.[16]

Recently, electrolytes based on organic/inorganic hybrid materials[22] and biopolymer materials, such as chitosan,[17] agar,[23] carrageen,[13] and gelatin[24] have been proposed with high conductivity and carrageenan,[13] chitosan,[25] xanthan gum[12] and agar-based systems[15,21,26] have been successfully applied in DSSCs. In 1988 Khare, N. applied an agar based electrolyte with a ferrous/ferric cyanide redox couple in a CdS electrochemical cell that exhibited results comparable to the liquid electrolyte.[27] Agarose has been successfully applied in DSSCs using polyiodine based electrolytes. However, in QDSSCs dextran,[14] as gelator, and a natural polysaccharide konjac glucomannan[28] as a polysulfide based hydrogel, have been developed. The obtained photovoltaic performance with liquid and polymer gel electrolytes were almost identical, the liquid being slightly higher, indicating that gelation has no adverse effect on the conversion efficiency. However, studies using agar with polysulfide electrolyte in QDSSCs still have not been reported.[19,29] Biopolymers are also relatively cheap, biodegradable and renewable, and most of the bio-macromolecules can dissolve inorganic salts or acids, making it possible to use them in polymer electrolytes.[17,30] Agar is one biopolymer material extracted from red seaweed. It is a mixture of two polysaccharides: agaropectin and agarose. Although both polymers share the same galactose-based backbone, agaropectin presents acidic side-groups such as sulfate and pyruvate, and agarose has a neutral charge. Fig. S1† illustrates the structure of agarose.[30] Agarose shows the ability to form a mechanically strong gel with a small amount of agarose. It is possible to use as gelator to obtain a solid system, keeping the ionic conductivity of the liquid electrolyte almost unaffected and assist in wetting the electrodes. It is considered a good and environment-friendly polymer matrix because of their rich hydroxyl groups in molecule structure, generating complexing sites. The conduction process occurs through the exchange of ions between complexed sites.[20,21,31]

In the present paper, agar-based gel electrolytes were prepared and applied in $CuInS_2$ and CdS QDSSCs. The counter electrodes such as reduced graphene oxide (RGO)–Cu_2S, brass and thin film Cu_xS were tested with this agar-based gel electrolyte. Impedance spectroscopy measurements were performed in order to determine the ionic conductivity of the electrolyte. The photovoltaic performance including long-term stability was evaluated and discussed to highlight the best solar cell device.

Results and discussion

Synthesis and characterization of $CuInS_2$ quantum dots and preparation of CdS semiconductor

Fig. 1 shows the absorption and photoluminescence spectra for the synthesized $CuInS_2$ QDs. $CuInS_2$ QDs synthesized in this study displays a broad absorption and emission feature and a large stokes shift indicating the presence of two optical transitions and defect-induced emission as reported previously.[33] $CuInS_2$ QDs were prepared using a slightly copper-deficient sample ([Cu] : [In] = 0.86 according to ICP) in order to obtain a higher photoluminescence quantum yield (Φ) as well as more absorption in the visible spectrum.[33] The Φ obtained was 0.085. In our previous work we found that $CuInS_2$ QDs with higher Φ exhibit better solar cell efficiency.[6]

The shape and size of the $CuInS_2$ QDs were determined by scanning transmission electron microscopy (STEM). STEM

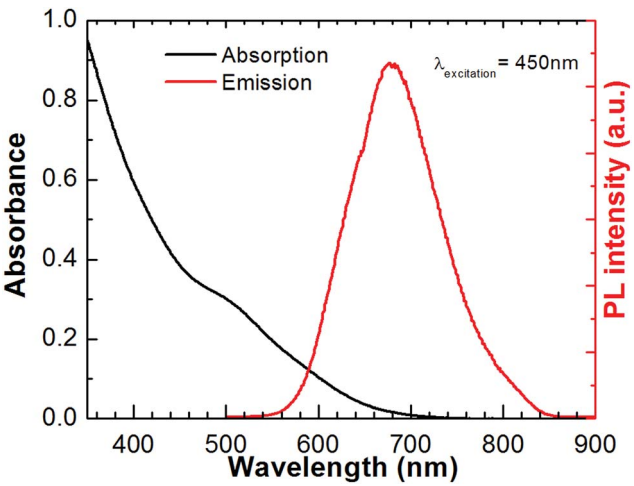

Fig. 1 Absorption and emission spectra for $CuInS_2$ QDs. Emission spectrum was recorded at 450 nm excitation wavelength in $CHCl_3$ solution.

analysis revealed that $CuInS_2$ QDs possess a pyramidal shape and size distribution of 2.9 ± 0.4 nm (Fig. 2A and B). The X-ray diffraction (XRD) patterns were scanned in the range of 20 to 85° as shown in Fig. 3. It shows five diffraction peaks at 28, 47, 55, 67 and 76° corresponding to indices (112), (204/220), (312), (400) and (316/322) lattice planes of a tetragonal chalcopyrite-like structure (JCPDS-75-0106).[34–36] There is no evidence of other secondary phases.

The deposition of CdS onto TiO_2 electrodes was performed by SILAR method. The preparation of CdS by SILAR method has already been described in literature.[37,38] It was used here for comparison purposes with this novel GPE electrolyte.

Preparation and characterization of agar-based polymer gel electrolyte

The preparation of agar-based gel electrolyte was made by dispersing 0.125 g of agar and 0.125 g of glycerol in 7.5 mL of water. This solution was constantly stirred and heated until boiling. The temperature was decreased to 60–70 °C, then 130 μL of formaldehyde was added while still stirring. Before application of the electrolyte in the QDSSCs, 2 mL of a 2 M Na_2S/S solution was added under stirring for 10–20 min. The ionic conductivity of agar-based polymer gel electrolyte was evaluated by Impedance Electrochemical Spectroscopy (IES) using an Autolab PGSTAT 302N Potentiostate over frequency range 100 Hz to 1 MHz. Fig. 4 shows the impedance plots for the agar-based gel electrolyte at room temperature. The intersection of the imaginary axis with the real axis provides the electrolyte bulk resistance (R_b). The ionic conductivity is then deduced using the relationship: $\sigma = l/(R_b A)$, where (σ) is ionic conductivity, l is the thickness of the electrolyte and A is the contact area between the electrolyte and the electrode. There is no existing capacitance component; the agar-based gel electrolyte shows only a resistive component at low frequency ranges which corresponds to the mass transport through the gel.[15] The agar-based electrolyte containing Na_2S/S showed resistance 32.15 ohm, from which we can determine an optimal result of ionic conductivity = 1.81×10^{-3} S cm^{-1}. This conductivity value can be compared to the conductivity value of liquid electrolyte (4.40×10^{-3} S cm^{-1}) usually applied in solar cells,[13] and being higher than previous results reported for an agar-based solid polymer electrolyte.[23]

In order to evaluate the thermal stability of the agar, thermogravimetric analysis (TGA) was performed. Fig. S2† shows the thermogravimetric curves from pure agar in the form of powder, and processed in the form of a membrane prepared with agar, glycerol and formaldehyde. From these results a slight weight loss of around 10% is recorded up to 150 °C in both samples. This mass loss event can be explained as a vaporization of residual water always present in the sample.[30,39] In the temperature range of 250–350 °C, an accentuated event reaching to 60% of mass loss occurs, which marks the degradation process of both samples. This degradation slowly continues as the temperature is increased to 800 °C with 10% of residue remaining. The processed sample (membrane) exhibits similar degradation to the plain agar, in which good thermal stability up to 250 °C can be highlighted. This thermal stability is suitable for application in solar cell preparation.

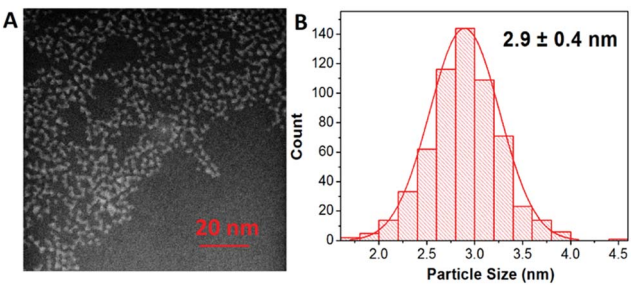

Fig. 2 (A) STEM image of $CuInS_2$ QDs showing the particles with pyramidal shape. (B) Size distribution of the particles with an average size of 2.9 nm.

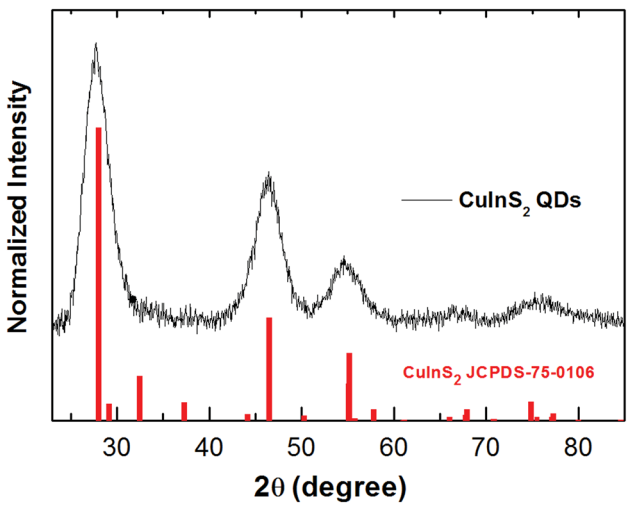

Fig. 3 X-ray diffraction pattern of $CuInS_2$ QDs and bulk pattern of chalcopyrite.

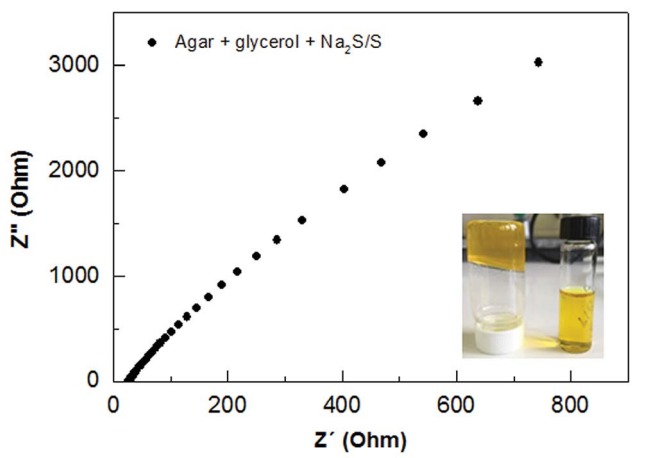

Fig. 4 Complex impedance plot for the agar-based gel electrolyte at room temperature.

Photovoltaic performance of CdS and $CuInS_2$-based solar cells

To evaluate the photovoltaic performance of CdS and $CuInS_2$-based solar cells, different electrolytes and counter electrodes were used. The photoanode was prepared by first depositing a layer of 20 nm TiO_2 nanoparticles (active layer) with an area of 0.20 cm^2 on fluorine-doped tin oxide (FTO) followed by a layer of 400 nm TiO_2 nanoparticles (scattering layer). It has been previously reported that the thickness of the active and scattering layer using doctor blade method is 11 ± 0.5 μm and 6 ± 0.5 μm, respectively.[36] Then, the active layer of TiO_2 was coated with CdS using SILAR method[40] with ten cycles of deposition or $CuInS_2$ QDs using an electrophoretic deposition (EPD) method. A DC voltage of 225 V cm^{-1} was applied between the TiO_2 film electrode and a FTO electrode immersed in QD suspensions. Loading of the $CuInS_2$ QDs onto mesoscopic TiO_2 film was optimized by tracking the absorption spectrum of the TiO_2/$CuInS_2$ film *versus* the time of EPD. Fig. S3† exhibits the absorption spectra of maximum loaded $CuInS_2$ photoanodes. These electrodes were subjected to two cycles of ZnS passivation layer using the SILAR method before assembling them in solar cells. A reduced graphene oxide (RGO)–Cu_2S composite[41] and Cu_xS/brass were used as the counter electrode for the CdS QDSSCs. The same reduced graphene oxide (RGO)–Cu_2S composite and a thin film layer of Cu_xS[42] (300 nm) were used as the counter electrode for the $CuInS_2$ QDSSCs. A liquid electrolyte (LE) employing a Na_2S/S solution and an agar-based gel polymer electrolyte (GPE) with Na_2S/S, both using a concentration of 0.42 M Na_2S/S.

Photovoltaic performance of the QDSSCs were measured under AM 1.5G simulated solar irradiation. Fig. 5 compares the Open Circuit Voltage, *J*–*V* characteristics and photocurrent stability of the $CuInS_2$ QDSSCs for the different electrolytes: liquid electrolyte (LE) or agar-based gel electrolyte (GPE) and different counter electrodes: graphene oxide (RGO)–Cu_2S composite (Cu_2S/RGO) or a thin film of Cu_xS. Two different counter electrodes were used for each photosensitizer (RGO and Cu_xS for $CuInS_2$ QDs and RGO and Cu-brass for CdS QDs) in order to test the GPE in the most common counter electrodes used in QDSSCs. We found that all of them work perfectly well with GPE opening the possibility of using this quasi-solid electrolyte with any counter electrode. The highest photocurrent was obtained for GPE, exhibiting a maximum short-circuit current density (J_{sc}) of 10.75 ± 0.87 mA cm^{-2} using Cu_2S/RGO as counter electrode and having an open-circuit voltage (V_{oc}) of 0.584 ± 0.018 V (Fig. 5B). As a result, the power conversion efficiency (PCE (η)) was highest for the QDSSCs employing GPE of 2.97 and 2.45%, from Cu_2S/RGO and Cu_xS counter electrode, respectively. It should be noted that the efficiencies for these cell using an agar based gel polymeric electrolyte are about factor of 0.3 and 0.07 higher than using a liquid electrolyte. Furthermore, we demonstrated that Cu_xS counter electrode may work as well as Cu_2S/RGO.

Fig. 6A compares the open circuit voltage, *J*–*V* characteristics and photocurrent stability of the CdS QDSSCs for the different electrolytes: liquid electrolyte (LE) or agar based gel electrolyte (GPE) and different counter electrodes: graphene oxide (RGO)–Cu_2S composite (Cu_2S/RGO) or brass (Cu_xS/brass). The highest

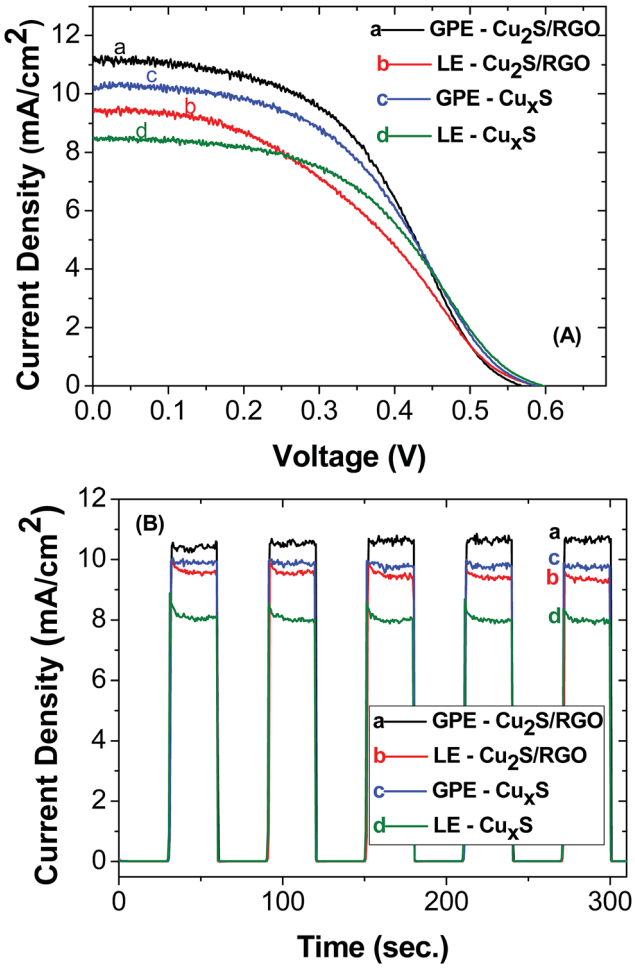

Fig. 5 Current–voltage characteristic (A) and photocurrent stability (B) of $CuInS_2$ QDSSCs. The electrolyte and counter electrode used in both experiments are shown in the inset.

photocurrent was obtained for GPE using Cu_2S/RGO as counter electrode, exhibiting a maximum short-circuit current density (J_{sc}) of 13.51 ± 0.85 mA cm^{-2} and an open-circuit voltage (V_{oc}) of 0.575 ± 0.003 V (Fig. 6B). As a result, the highest power conversion efficiency (PCE (η)) was 2.98 and 2.77% for the solar cells employing GPE with Cu_2S/RGO and Cu_xS/brass counter electrode, respectively. It should be noted that the efficiencies for these cell using an agar-based gel polymeric electrolyte are about factor of 0.06 and 0.31 higher than using a liquid electrolyte. The solar cell parameters are summarized in Table 1.

The photovoltaic parameters of the QDSSCs with GPE were enhanced by the introduction of a polymer into the electrolyte. According to Table 1, which shows a summary of photovoltaic parameters for all cells, V_{oc} is observed to be quite similar between solar cells using LE and GPE considering the error of the three solar cells tested for each sample. This observation is in agreement with the fact that both solar cells, LE and GPE, are using the same redox couple. The most relevant parameter affected by the electrolyte phase is J_{sc}, which is clearly higher for all samples containing GPE. This last factor is responsible for the enhancement of the photovoltaic efficiency. This polymer

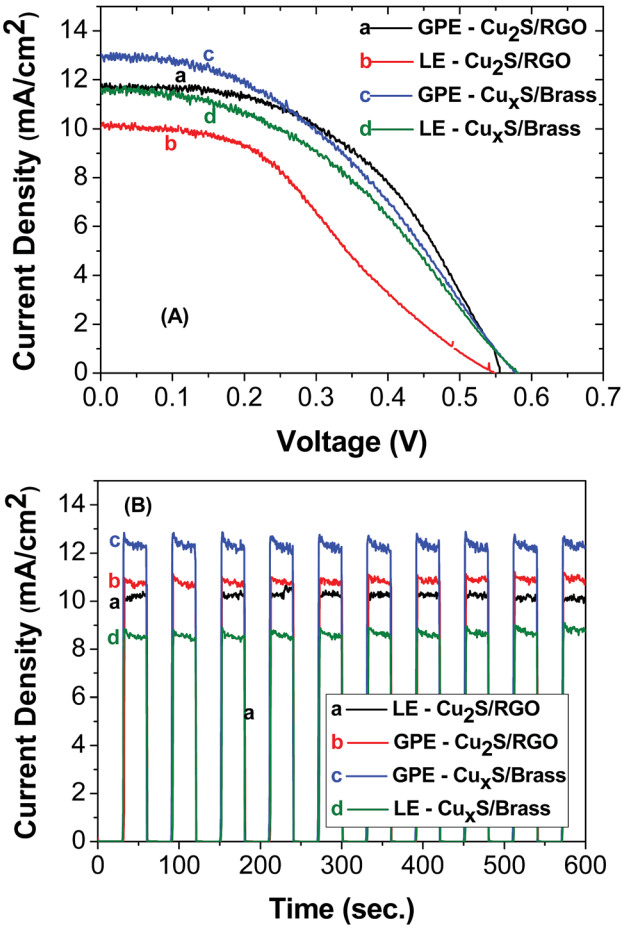

Fig. 6 Current–voltage characteristic (A) and photocurrent stability (B) of CdS QDSSCs. The electrolyte and counter electrode used in both experiments are shown in the inset.

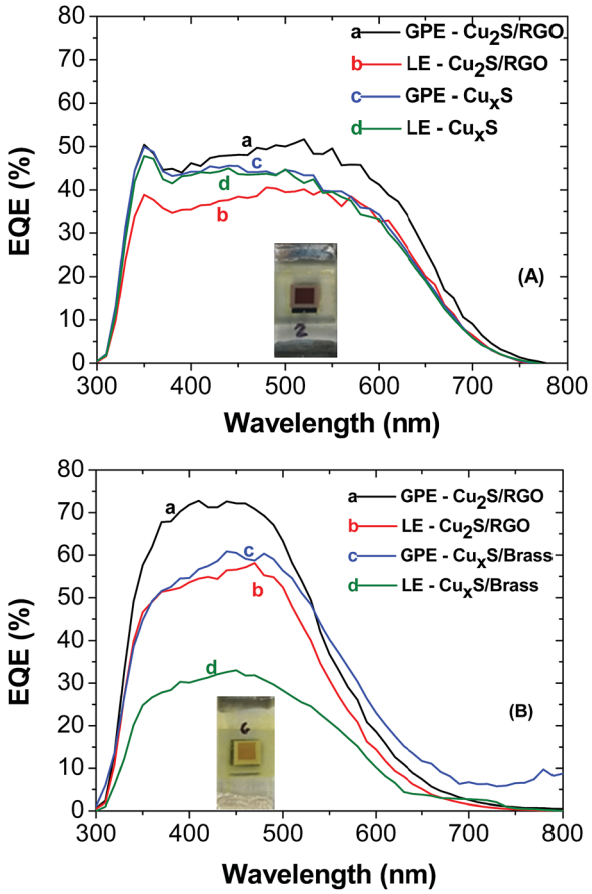

Fig. 7 IPCE curves of $CuInS_2$ QDSSCs (A) CdS QDSSCs (B). The electrolyte and counter electrode used in both samples are shown in the inset.

improves the dissociation of Na_2S, by coordination of Na^+ with the agar hydroxyl groups, resulting in an increase in S^{2-}/S_n^{2-} content in the electrolyte. A higher concentration of S^{2-}/S_n^{2-} will accelerate the regeneration of the oxidized quantum dot and the accumulated electrons in TiO_2 *via* charge injection from excited quantum dot.[20,43] Another factor is that a water based polysulfide electrolyte does not have a good permeation into TiO_2 mesoporous film or a good contact between electrolyte and QDs, while with an agar the good permeation of gel electrolyte may contribute to the better photovoltaic performance.[19,20] Higher PCE values were also obtained with agar as a solidified electrolyte in DSSCs.[25] These promising results suggest new potential towards environmental friendly materials for new generation photovoltaics.

Incident photon-to-carrier conversion efficiency (IPCE) or external quantum efficiency (EQE) represents the percentage of incident photons that are converted to charge carriers and collected at the electrode surface. The IPCE spectra of $CuInS_2$ QDSSCs is shown in Fig. 7A. The samples with the gel electrolyte

Table 1 Photovoltaic parameter of CdS and $CuInS_2$ solar cells made with different counter electrode and electrolyte[a]

Sensitizer/CE	Electrolyte	V_{oc} (V)	J_{sc} (mA cm^{-2})	FF	η (%)
$CuInS_2/Cu_2S$–RGO	LE	0.579 ± 0.018	8.91 ± 0.50	0.39 ± 0.05	2.06 ± 0.17
$CuInS_2/Cu_2S$–RGO	GPE	0.584 ± 0.018	10.75 ± 0.87	0.47 ± 0.06	2.97 ± 0.06
$CuInS_2/Cu_xS$	LE	0.597 ± 0.003	8.40 ± 0.15	0.45 ± 0.01	2.28 ± 0.10
$CuInS_2/Cu_xS$	GPE	0.577 ± 0.013	9.26 ± 0.88	0.46 ± 0.01	2.45 ± 0.27
CdS/Cu_2S–RGO	LE	0.587 ± 0.008	10.95 ± 0.85	0.43 ± 0.04	2.80 ± 0.03
CdS/Cu_2S–RGO	GPE	0.575 ± 0.003	13.51 ± 0.85	0.38 ± 0.01	2.98 ± 0.11
CdS/Cu_xS-brass	LE	0.506 ± 0.070	9.74 ± 0.80	0.41 ± 0.06	1.88 ± 0.21
CdS/Cu_xS-brass	GPE	0.553 ± 0.007	12.40 ± 0.98	0.41 ± 0.09	2.77 ± 0.39

[a] Results are tabulated and calculated for three tested cells.

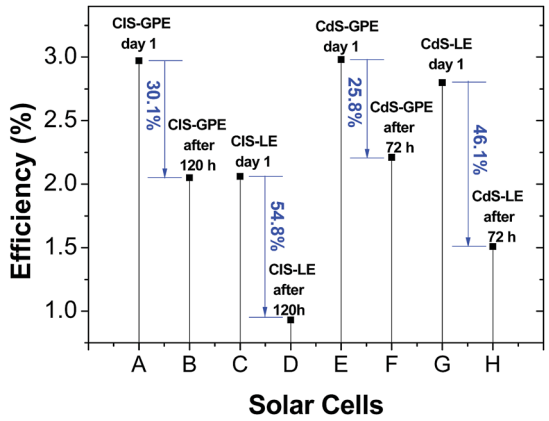

Fig. 8 Electrolyte stability for QDSSCs.

exhibit greater incident photon to current conversion efficiency than the liquid electrolyte with a maximum IPCE of 52% at 520 nm. The IPCE spectra shown in the Fig. 7B for CdS with the same electrolytes exhibits greater incident photon to current conversion efficiency with a maximum IPCE of 71.7% at 440 nm. In both cases we can observe an improvement to the light absorption in the cells prepared with agar-based gel polymer electrolyte, as it exhibits better electron collecting and transport properties than the liquid electrolyte, which proved that the agar based gel electrolyte significantly improved the efficiency of the cell.

Even though we obtained a lower photovoltaic efficiency than other QDSSCs devices, our results show preliminary and promising results using quasi-solid electrolytes. We believe that the solar cell efficiency may be increased by changing for example the long-chain capping ligand in $CuInS_2$ QDs for shorter ligands as was demonstrated in a previous work.[42] Shorter ligands help to increase the concentration of the dye in the mesoporous TiO_2 and improve the electron transfer process between the photosensitizer and TiO_2. Another strategy to improve the photovoltaic performance is using another counter electrode such as CoS–CuS hybrid structure, which has been shown to obtain higher photovoltaic performance than bare CoS or CuS.[44]

Stability after storage

Fig. S4† compares the *J*–*V* curves and photocurrent stability of the solar cells employing CdS (being stored for 72 hours) and $CuInS_2$ (being stored for 120 hours), both with RGO/Cu_2S as counter electrode. Each cell was stored under dark at room temperature inside sealed plastic bottles. For both cells employing LE we can observe a decrease in the short-circuit current density (J_{sc}) about a factor of 0.25 and 0.28 (CdS and CIS respectively) after storage. For both cells employing GPE we can observe the best stability for the short-circuit current density (J_{sc}) decreasing about a factor of 0.20 and 0.09 after storage. From the results obtained, it is evident that the application of a gel polymer electrolyte in substitution of a conventional liquid electrolyte improves the device performance and shows a longer-term stability.

Under such conditions, the water content in both electrolytes is expected to decrease due to evaporation. Indeed, the efficiency of the solar cells employing a liquid electrolyte (LE) decreases drastically by 55% (from 2.06% to 0.93%) after 120 hours in $CuInS_2$ QDSSCs, and decreased about 46% (from 2.80% to 1.51%) after 72 hours in CdS QDSSCs. On the other hand, the solar cell efficiency employing GPE under the same conditions decrease in 30.1% (from 2.97% to 2.05%) and 25.8% (from 2.98% to 2.21%) for $CuInS_2$ and CdS, respectively (Fig. 8).

The results indicate that the cells prepared using GPE enhanced long-term stability, which is an important requirement to practical application of liquid-junction solar cells, and still remains a challenge.[45] The possible reasons for this result are that liquid electrolytes have several problems, such as leakage, volatilization of the solvent, and possible desorption of the attached sensitizers. Using agar as gelator in electrolyte has advantages such as higher power conversion efficiency and higher longevity of cell performance by mitigating the potential instability against solvent leakage and evaporation.[15,21] This can be attributed to the strong affinity between polymer matrix and solvent.[28] However we believe that polysulfide oxidation, QDs surface oxidation and its desorption from TiO_2 in both cells results in photovoltaic performance small decrease in long-term, which still remains a challenge to obtain excellent stability.[5,46] Table 2 summarizes the photovoltaic performance after storage.

Conclusions

An agar-based polymer gel electrolyte has been developed and successfully applied in $CuInS_2$ and CdS QDSSCs. The solar cells were fabricated using $CuInS_2$ quantum dots deposited on TiO_2 photoanodes by electrophoretic deposition (EPD) and CdS semiconductor deposition on TiO_2 photoanodes by ten cycles of successive ionic layer adsorption and reaction (SILAR) with reduced graphene oxide (RGO)–Cu_2S and Cu_xS as counter electrodes.

Table 2 Photovoltaic parameters of CdS and $CuInS_2$ QDSSCs made with Cu_2S–RGO counter electrode measured after 72 and 120 hours, respectively[a]

Sensitizer – hours	Electrolyte	V_{oc} (V)	J_{sc} (mA cm^{-2})	FF	η (%)
$CuInS_2$ – 120	LE	0.545 ± 0.017	7.02 ± 0.23	0.25 ± 0.04	0.93 ± 0.11
$CuInS_2$ – 120	GPE	0.548 ± 0.020	9.74 ± 0.72	0.38 ± 0.03	2.05 ± 0.41
CdS – 72	LE	0.463 ± 0.038	8.54 ± 1.79	0.38 ± 0.16	1.51 ± 0.20
CdS – 72	GPE	0.559 ± 0.015	10.63 ± 2.89	0.45 ± 0.15	2.21 ± 0.09

[a] Results are tabulated and calculated for three tested cells.

$CuInS_2$ based QDSSCs with agar-based gel polymeric electrolyte exhibit IPCE (maximum IPCE = 51.7% at 520 nm), short circuit current (J_{sc} = 10.75 mA cm^{-2}), power conversion efficiency (η = 2.97%). The CdS based QDSSCs with the same electrolyte exhibit greater incident photon to current conversion efficiency (maximum IPCE = 71.7% at 440 nm), short circuit current (J_{sc} = 13.91 mA cm^{-2}), and power conversion efficiency (η = 2.98%).

The photovoltaic efficiency for the CdS solar cells employing GPE for Cu_2S/RGO and Cu_xS/brass counter electrode are about a factor of 0.06 and 0.31 higher than using a liquid electrolyte, respectively. For the CIS solar cells employing GPE for Cu_2S/RGO and Cu_xS counter electrode are about factor of 0.3 and 0.07 higher than using a liquid electrolyte, respectively. Such results are promising and suggest new potential material for solid/gel electrolytes in QDSSCs.

Both cells exhibited significantly enhanced stability, compared to the liquid electrolyte. These results indicate that the agar-based gel electrolyte exhibits almost the same conductivity as the liquid electrolyte. The electron transport was faster in the gel-electrolyte than the liquid one. Finally, since the gel network can create better sealing and avoid the leakage of solvent, this electrolyte has been identified as being a suitable material for practical photovoltaic devices.

Experimental

Materials

Copper(I) iodide (Alfa Aesar, puratronic, 99.998%), indium(III) acetate (Alfa Aesar, 99.99%), 1-dodecanethiol (Aldrich, ≤98%), toluene (Fisher Scientific, certified ACS grade), methanol (Fisher Scientific, certified ACS grade), chloroform (AMRESCO, biotechnology grade), $TiCl_4$ (Alfa Aesar, puratronic, 99.0%) and agar (Sigma-Aldrich) were used without purification. FTO glass plates from Pilkington (TEC-7), TiO_2 (Solaronix Ti Nanoxide T/SP, particle size ~ 20 nm), TiO_2 (CCIC, PST-400C, particle size ~ 400 nm).

Synthesis of $CuInS_2$ quantum dots

$CuInS_2$ (CIS) QDs were synthesized using a previously reported heating up method.[32] In brief, 0.7 mmol of CuI and 1 mmol of $In(Ac)_3$ were employed as precursors, and an excess of 1-dodecanethiol (1-DDT) was used as solvent, S donor, and capping ligand. Under vacuum, the reaction was heated for 30 min at 100 °C, and then the temperature was raised to 200 °C for 30 min. The as-synthesized CIS QDs were then washed by dispersing and precipitating the QDs with toluene and methanol, respectively. CIS QDs were stored in N_2 purged toluene until further characterization.

Quasi-solid electrolyte preparation

In order to prepare the quasi-solid electrolyte 0.125 g of agar (Aldrich®) and 0.125 g of glycerol (as a plasticizer), was dispersed in 7.5 mL of DI water and heated under magnetic stirring for a few minutes up to boiling to complete dissolution. Next, the solution was cooled down to 60 °C and 130 μL of formaldehyde (as a cross-linking agent) and 2 mL of a 2.0 M Na_2S/S polysulfide solution were added to this solution under stirring.

Photoanode preparation

Fluorine-doped tin oxide (FTO) glass plates from Pilkington (TEC-7) were cleaned in soap solution using an ultrasonic bath for 30 min and washed in ethanol for 15 min. Three layers of TiO_2 were deposited on FTO: a blocking layer, an active layer, and a scattering layer. The blocking layer was deposited by immersing the plates in 40 mM $TiCl_4$ aqueous solution at 70 °C for 30 min and washed with DI water and ethanol. The active TiO_2 layer (Solaronix Ti Nanoxide T/SP, particle size ~ 20 nm) was coated on top of the blocking layer by doctor blade technique. The film was dried at 80 °C for 1 h and then annealed at 400 °C, 450 °C and 500 °C for 15 min at each temperature. A scattering layer of TiO_2 (CCIC, PST-400C, particle size ~ 400 nm) was deposited on top of the active layer by doctor blade printing. The TiO_2 electrodes were further dried at 80 °C and then annealed at 400 °C, 450 °C and 500 °C for 15 min each temperature. Finally, the electrodes were treated again with $TiCl_4$ at 70 °C for 30 min and sintered at 500 °C for 30 min. The counter electrodes (CEs) were prepared by doctor blading Cu_2S–RGO as reported earlier.[41] Cu_xS counter electrodes were prepared by depositing a thin film (300 nm) of copper metal on a glass/FTO substrate, then it was immersed in a polysulfide solution (2 M Na_2S/S) for 30 minutes.[42] A brass electrode was prepared immersed in hydrochloric acid at 70 °C for 10 min, and then, the treated brass was dipped into polysulfide aqueous solution (2 M Na_2S/S) for 5 min.[47] The solar cells were fabricated by sandwiching the photoanode and counter electrodes using parafilm as spacer and a drop of redox electrolyte (0.42 M of S^{2-}, 0.42 M of S in water, or dispersing 2 mL of a polysulfide solution, 2.0 M Na_2S/S, in 7.5 mL of agar gel). The typical electrode area was 0.20 cm^2 for regular solar cells and 0.5 cm^2 for solar cells with no scattering layer. ImageJ software was used to determine the precise area of the electrodes.

Electrophoretic deposition (EPD)

EPD was used to sensitize the FTO/TiO_2 photoanodes with $CuInS_2$. A TiO_2 photoanode and a blank piece of FTO glass were immersed in a cuvette and kept at a distance of 0.4 cm. A dispersion of QDs in $CHCl_3$ was added in the cuvette, and a bias voltage of 225 V cm^{-1} was applied between the TiO_2 photoanode and FTO for different period of times to deposit the QDs onto the mesoporous TiO_2 electrode, which was connected to the positive terminal of the power supply unit.

Successive ionic layer adsorption and reaction (SILAR)

The deposition of CdS onto TiO_2 electrodes was performed by SILAR method. A $Cd(NO_3)_2$ (0.1 M) solution in methanol and a Na_2S (0.1 M) solution in methanol : water (1 : 1) were used as cationic and anionic sources, respectively. Each cycle of SILAR consists of successive immersion of the TiO_2 electrode in metal ion and sulfide anion solutions for 1 min and washing between each step. Ten cycles were applied for the CdS/TiO_2 photoanodes.

Two cycles of deposition of ZnS onto the CdS/TiO_2 and $CuInS_2/TiO_2$ photoanodes were performed by SILAR method, in these cases a $Zn(NO_3)_2$ (0.1 M) solution in methanol and Na_2S (0.1 M) in a mixture of methanol and water (1 : 1) were used as cationic and anionic sources, respectively. Each cycle of SILAR consists of successive immersion of the TiO_2 electrode in metal ion and sulfide anion solutions for 1 min and washing between each step.

Material characterization

Optical measurements. UV-visible absorption spectra were collected using a Varian Cary 50 Bio spectrophotometer. Steady state photoluminescence spectra were recorded using a Horiba FluoroLog spectrometer with a 450 nm long pass filter to exclude scattering from the excitation source. Transmission electron microscope (TEM) images were collected using a TITAN 80–300 electron microscope at an accelerating voltage of 300 kV. The samples for TEM were prepared by dropping a diluted solution of $CuInS_2$ QDs into a carbon coated nickel grid and dried under vacuum overnight. X-ray diffraction (XRD) measurement were performed by using a Bruker D8 X-ray diffractometer with scan rate of 2° min^{-1} over 2θ values of 20–85° and employing Cu Kα radiation ($\lambda = 1.5406$ Å).

Impedance electrochemical spectroscopy (IES). Impedance spectroscopy measurements were used to determine the electrolyte ionic conductivity and its frequency behavior. The measurements were carried out using an Autolab 302 instrument equipped with a FRA2 module, with amplitude of 5 mV and in the 102–106 Hz frequency range, with cells fabricated sandwiching the gel electrolyte between two pieces of FTO/glass with parafilm as spacer, ImageJ software was used to determine the precise area and the thickness of gel electrolytes was determined using a digital caliper JOMARCA 205509.

Thermogravimetric analysis (TGA). Thermogravimetric analysis (TGA) was carried out using a SHIMADZU TGA-50 equipment in the 25–800 °C temperature range under a nitrogen flow (50 mL min^{-1}) at a heating rate of 10 °C min^{-1}.

Photoelectrochemical measurements. Photoelectrochemical measurements were carried out with a sandwich cell configuration consisting of $CuInS_2$ or CdS sensitized TiO_2 photoanode, Cu_2S/RGO or Cu_xS thin film deposited on FTO electrode, or brass as cathode (see ref. 32 for preparation of the Cu_2S/RGO cathode) and sulfide/polysulfide electrolyte. The photovoltaic performances of QDSSCs were evaluated using a PARStat 2273 (Princeton Applied Research) potentiostat. The illumination source was a 300 W Xe lamp (Oriel) with a global AM 1.5 filter. The solar cells were positioned to receive incident power energy of 1 sun intensity (100 mW cm^{-2}). The incident photon-to-charge carrier generation efficiency (or external quantum efficiency) at different wavelengths was measured using Newport Oriel QE/IPCE Measurement Kit with Silicon Detector.

Acknowledgements

The authors thank Dr Prashant Kamat and DOE for providing the facilities and support. The research described herein was supported by the Division of Chemical Sciences, Geosciences, and Biosciences, Office of Basic Energy Sciences of the U.S. Department of Energy, through award DE-FC02-04ER15533. This is contribution number NDRL No. #5106 from the Notre Dame Radiation Laboratory. ER thanks CNPq (Ciência sem Fronteiras) for the Postdoctoral Fellowship (GDE 201293/2014-5). DHJ would like to thank to Comisión Nacional de Investigación Científica y Tecnológica (CONICYT) for the Becas Chile Scholarship, code 72110038.

References

1 P. V. Kamat, *J. Phys. Chem. C*, 2007, **111**, 2834.
2 L. Li, X. Yang, J. Gao, H. Tian, J. Zhao, A. Hagfeldt and L. Sun, *J. Am. Chem. Soc.*, 2011, **133**, 8458.
3 S. Rühle, M. Shalom and A. Zaban, *ChemPhysChem*, 2010, **11**, 2290.
4 P. V. Kamat, *J. Phys. Chem. Lett.*, 2013, **4**, 908.
5 D. A. Hines and P. V. Kamat, *ACS Appl. Mater. Interfaces*, 2014, **6**, 3041.
6 D. H. Jara, S. J. Yoon, K. G. Stamplecoskie and P. V. Kamat, *Chem. Mater.*, 2014, **26**, 7221.
7 R. Salazar, A. Delamoreanu, C. Levy-Clement and V. Ivanova, *European Materials Research Society Conference Symposium: Advanced Inorganic Materials and Concepts for Photovoltaics*, 2011, 10, DOI: 10.1016/j.egypro.2011.10.164.
8 M. R. Kim and D. Ma, *J. Phys. Chem. Lett.*, 2015, **6**, 85.
9 H. Choi, R. Nicolaescu, S. Paek, J. Ko and P. V. Kamat, *ACS Nano*, 2011, **5**, 9238.
10 A. Polman, M. Knight, E. C. Garnett, B. Ehrler and W. C. Sinke, *Science*, 2016, **6283**, 307.
11 P. V. Kamat, *Acc. Chem. Res.*, 2012, **45**, 1906.
12 S. J. Park, K. Yoo, J.-Y. Kim, J. Y. Kim, D.-K. Lee, B. Kim, H. Kim, J. H. Kim, J. Cho and M. J. Ko, *ACS Nano*, 2013, **7**, 4050.
13 M. Kaneko, T. Hoshi, Y. Kaburagi and H. Ueno, *J. Electroanal. Chem.*, 2014, **572**, 21.
14 H.-Y. Chen, L. Lin, X.-Y. Yu, K.-Q. Qiu, X.-Y. Lü, D.-B. Kuang and C.-Y. Su, *Electrochim. Acta*, 2013, **92**, 117.
15 S. S. Alias and A. A. Mohamad, *Ionics*, 2013, **19**, 1185.
16 O. A. Ileperuma, *Mater. Technol.*, 2013, **28**, 65.
17 A. Pawlicka, M. Danczuk, W. Wieczorek and E. Zygadlo-Monikowska, *J. Phys. Chem. A*, 2008, **112**, 8888.
18 Z. Seidalilir, R. Malekfar, H.-P. Wu, J.-W. Shiu and E. W.-G. Diau, *ACS Appl. Mater. Interfaces*, 2015, **7**, 12731.
19 M. S. Su'ait, M. Y. A. Rahman and A. Ahmad, *Sol. Energy*, 2015, **115**, 452.
20 Y. Yang, H. Hu, C.-H. Zhou, S. Xu, B. Sebo and X.-Z. Zhao, *J. Power Sources*, 2011, **196**, 2410.
21 R. Singh, N. A. Jadhav, S. Majumder, B. Bhattacharya and P. K. Singh, *Carbohydr. Polym.*, 2013, **91**, 682.
22 D. Sygkridou, A. Rapsomanikis and E. Stathatos, *Sol. Energy Mater. Sol. Cells*, 2017, **159**, 600.
23 E. Raphael, C. O. Avellaneda, M. A. Aegerter, M. M. Silva and A. Pawlicka, *Mol. Cryst. Liq. Cryst.*, 2012, **554**, 264.
24 D. F. Vieira, C. O. Avellaneda and A. Pawlicka, *Electrochim. Acta*, 2007, **53**, 1404.
25 S. A. Mohamad, R. Yahya, Z. A. Ibrahim and A. K. Arof, *Sol. Energy Mater. Sol. Cells*, 2007, **91**, 1194.

26 M. Bidikoudi, D. Perganti, C. Karagianni and P. Falaras, *Electrochim. Acta*, 2015, **179**, 228.
27 N. Khare, *J. Power Sources*, 1988, **24**, 121.
28 S. Wang, Q.-X. Zhang, Y.-Z. Xu, D.-M. Li, Y.-H. Luo and Q.-B. Meng, *J. Power Sources*, 2013, **224**, 152.
29 P. Wang, S. M. Zakeeruddin, J. E. Moser, M. K. Nazeeruddin, T. Sekiguchi and M. Gratzel, *Nat. Mater.*, 2003, **2**, 402.
30 E. Raphael, C. O. Avellaneda, B. Manzolli and A. Pawlicka, *Electrochim. Acta*, 2010, **55**, 1455.
31 K. Suzuki, M. Yamaguchi, M. Kumagai, N. Tanabe and S. Yanagida, *C. R. Chim.*, 2006, **9**, 611.
32 L. Li, A. Pandey, D. J. Werder, B. P. Khanal, J. M. Pietryga and V. I. Klimov, *J. Am. Chem. Soc.*, 2011, **133**, 1176.
33 D. H. Jara, K. G. Stamplecoskie and P. V. Kamat, *J. Phys. Chem. Lett.*, 2016, **7**, 1452.
34 H. Z. Zhong, S. S. Lo, T. Mirkovic, Y. C. Li, Y. Q. Ding, Y. F. Li and G. D. Scholes, *ACS Nano*, 2010, **4**, 5253.
35 L. Li, N. Coates and D. Moses, *J. Am. Chem. Soc.*, 2010, **132**, 22.
36 P. K. Santra, P. V. Nair, K. G. Thomas and P. V. Kamat, *J. Phys. Chem. Lett.*, 2013, **4**, 722.
37 Y. F. Nicolau, *Appl. Surf. Sci.*, 1985, **22–3**(5), 1061.
38 M. A. Becker, J. G. Radich, B. A. Bunker and P. V. Kamat, *J. Phys. Chem. Lett.*, 2014, **5**, 1575.
39 G. O. Machado, R. E. Prud'homme and A. Pawlicka, *e-Polym.*, 2007, **7**, 1335.
40 D. R. Baker and P. V. Kamat, *Adv. Funct. Mater.*, 2009, **19**, 805.
41 J. G. Radich, R. Dwyer and P. V. Kamat, *J. Phys. Chem. Lett.*, 2011, **2**, 2453.
42 H. McDaniel, N. Fuke, N. S. Makarov, J. M. Pietryga and V. I. Klimov, *Nat. Commun.*, 2013, **4**, 2887.
43 D. Cahen, G. Hodes, M. Grätzel, J. F. Guillemoles and I. Riess, *J. Phys. Chem. B*, 2000, **104**, 2053.
44 L. Givalou, M. Antoniadou, D. Perganti, M. Giannouri, C. S. Karagianni, A. G. Kontos and P. Falaras, *Electrochim. Acta*, 2016, **210**, 630.
45 A. Hinsch, J. M. Kroon, R. Kern, I. Uhlendorf, J. Holzbock, A. Meyer and J. Ferber, *Prog. Photovoltaics*, 2001, **9**, 425.
46 H. K. Jun, M. A. Careem and A. K. Arof, *Int. J. Photoenergy*, 2013, **2013**, 10.
47 H. K. Jun, M. A. Careem and A. K. Arof, *Nanoscale Res. Lett.*, 2014, **9**(1), 1.